Archives of Hydro-Engineering and Environmental Mechanics
Vol. 57 (2010), No. 3-4, pp. 243–260

A Study on the Pull-out Resistance of Dynamically Driven Nails and the Cavity Expansion Method

Andrzej Sawicki

Institute of Hydro-Engineering, Polish Academy of Sciences, Kościerska 7, 80-328 Gdańsk, Poland,
e-mail: as@ibwpan.gda.pl

(Received January 17, 2011; revised February 16, 2011)

Abstract

The problem is how to assess normal stresses around dynamically driven nails. Pull-out tests show that these stresses are much higher than it would follow from classical analyses. Therefore, an analysis of the cavity expansion method was applied to study this problem. It was shown that the cavity expansion method, widely applied in soil mechanics, suffers from many shortcomings. It was also shown that this method is not closely related to cone penetration tests, nor to the technology of dynamic soil nailing.

Key words: soil nailing, cavity expansion, cone penetration tests

1. Introduction

The dynamic soil nailing differs from the classical technology, in which nails are introduced into holes drilled in the soil mass, and then the whole system is grouted. As a result, a kind of composite structure is created, consisting of the nail, surrounding cement mixture, and natural soil. This technique does not essentially change the stress state in the soil mass, except perhaps for local disturbances. A different situation occurs when the nails are introduced dynamically, i.e. by hammering or vibrations, and when the soil is not excavated but rather compacted around the nail. It appears that the nailing technique may influence the stress state around the nail, but this problem has not been sufficiently investigated, and no conclusions of practical importance can be drawn. Some discussion of these problems will be presented in this paper.

The pull-out resistance of a nail can be estimated using a basic scheme shown in Fig. 1. The pulling-out force F should simply resist the shearing stresses τ around the nail. The maximum value of this force at the beginning of the pull-out process is the following:

$$F_{\max} = \tau S L, \tag{1}$$

where:

L – nail's length,
S – nail's circumference.

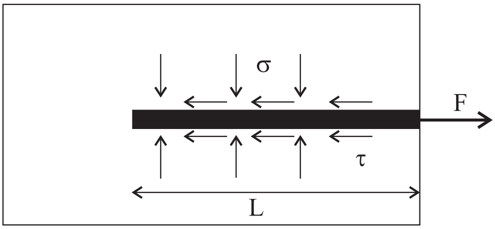

Fig. 1. Simple scheme for estimating a nail's pull-out resistance

During the movement of the nail with respect to the soil, there is $\tau = \mu\sigma$, where μ is a coefficient of friction between the nail and the soil. It is obvious that the pull-out resistance strongly depends on the normal stress σ. Note that this simple analysis does not take into account many details, such as the cross-sectional shape of the nail, non-uniform distribution of stresses, etc. The normal stress is usually calculated from the own weight of soil above the nail (geostatic stress).

However, in the case of dynamically driven nails the above simple procedure does not apply. Some in-situ investigations, performed in Gdańsk during construction of excavations in urban areas, showed that the pull-out resistance of L-shaped nails driven by vibrations was about 4 times larger than it would follow from the simple procedure described above. One possible explanation of this phenomenon is that the process of driving the nails in had generated some additional normal stresses around them.

In order to verify this hypothesis, laboratory investigations were performed in the experimental setup shown in Fig. 2. A cylindrical steel nail of 16 mm in diameter was hammered into a sand-filled closed cylindrical steel tube of 107 mm in diameter. Unfortunately, the process of driving the nail in could not be controlled. Then the nail was pulled out. A simple analysis, using Eq. (1), showed that radial stresses generated around the nail should be of the order of 5 MPa, Sawicki and Kulczykowski (2010).

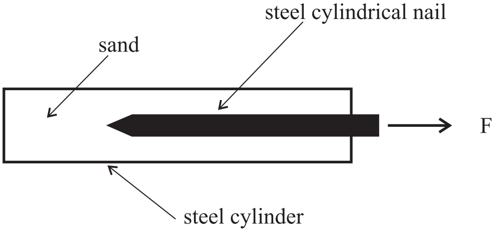

Fig. 2. Experimental setup

The above experiments support the hypothesis that the process of dynamic driving generates additional radial stresses between the nail and the soil. Note that the experimental nail has a conical edge, so the cone penetration during driving is coupled with cavity expansion, which is supported by independent opinions. For example: "Due to similar mechanical action generated by cavity expansion and cone penetration .... cavity expansion theory has been used with considerable success in the interpretation of .... in situ soil tests.", cf. Yu (2000), page 209. An interesting question is whether the cavity expansion method can make it possible to determine radial stresses generated by dynamic nailing.

2. Cavity Expansion Method and Its Shortcomings

The cavity expansion method has received a great deal of attention in soil mechanics as it can be applied to solve various problems of practical importance, including in-situ testing methods (penetrometers), pile foundations, underground excavations and tunneling, underground explosions, etc., see Bigoni and Laudiero (1989), Carter et al (1986), Salgado et al (1997), Su and Liao (2001). An advantage of cavity expansion methods is that they often enable researchers to find analytical solutions of the problems considered. An extensive treatment of these methods is presented in Yu (2000), where most relevant publications are also quoted. Sawicki and Kulczykowski (2010) have tried to apply a simple cavity expansion method to analyse the problem of interaction between a dynamically driven nail and the surrounding soil, but with limited success. In this paper a more detailed analysis of this problem will be presented.

Consider an expansion of a cylindrical cavity in an infinite medium caused by the internal pressure p, as shown in Fig. 3. The initial radius of the cavity is a. The pressure p increases the cavity radius to b. The plane strain and axi-symmetric conditions are assumed. For the sake of simplicity, an initial stress-free condition in the medium surrounding the cavity is also assumed. On the other hand, the experiments mentioned in the previous section were performed under almost stress-free initial conditions. The pressure p generates radial and circumferential stresses in the medium, designated as σ_r and σ_Θ respectively. The soil mechanics sign convention is applied, where the plus sign denotes compression.

The stresses should satisfy the following equilibrium equation:

$$\frac{\partial \sigma_r}{\partial r} + \frac{\sigma_r - \sigma_\Theta}{r} = 0, \tag{2}$$

with the boundary condition $\sigma_r(r = a) = p$. The following functions satisfy these requirements:

$$\sigma_r = p\left(\frac{a}{r}\right)^2, \tag{3}$$

$$\sigma_\Theta = -p\left(\frac{a}{r}\right)^2. \tag{4}$$

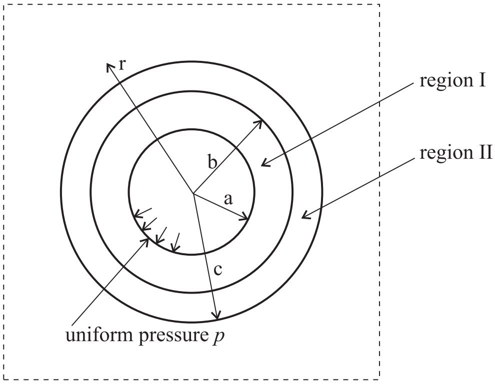

Fig. 3. Expansion of cylindrical cavity in infinite medium

Note that these stresses disappear when $r \to \infty$, as it should be. Eqs. (3) and (4) are well known in applied mechanics, see Hill (1950) or Timoshenko and Goodier (1951). In the case of an elastically linear medium, they also satisfy the strain compatibility condition. Therefore, from a formal point of view, Eqs. (3) and (4) properly describe the stress state in a medium surrounding an expanding cavity. However, if this medium consists of granular matter, such as sand, the above solution raises some questions.

In the case of an initially unstressed granular medium, Eq. (4) leads to negative (extension) circumferential stresses, which cannot be accepted in the case of granular materials, for which $\sigma_\Theta \geq 0$. If these stresses are imposed onto some initial stress state, one can accept this formal solution, provided that the Coulomb-Mohr yield condition is not violated. In the case of an initially unstressed medium, this condition is violated from the very beginning. In the case considered, the Coulomb-Mohr yield condition has the following form:

$$\sigma_r - \sigma_\Theta - (\sigma_r + \sigma_\Theta)\sin\varphi \leq 0, \tag{5}$$

where φ is the angle of internal friction.

Substitution of Eqs. (3) and (4) into Eq. (5) leads to contradiction. This means that the above solution cannot be applied to granular soils in initially stress-free conditions. The stress path followed during the cavity expansion is outside the statically admissible region in the stress space, as shown in Fig. 4.

In the case when the constant hydrostatic pressure p_0 acts throughout the soil before cavity expansion, the following stresses describe the problem:

$$\sigma_r = p_0 + (p - p_0)\left(\frac{a}{r}\right)^2, \tag{6}$$

$$\sigma_\Theta = p_0 - (p - p_0)\left(\frac{a}{r}\right)^2. \tag{7}$$

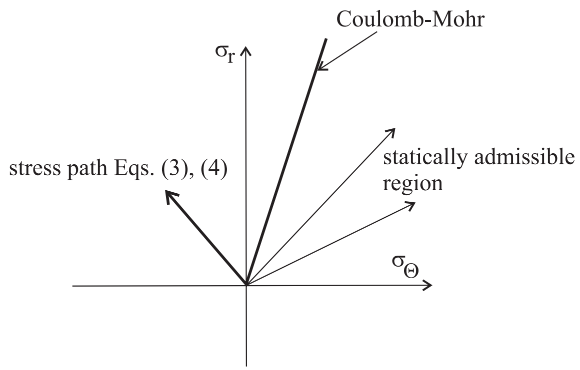

Fig. 4. Stress path defined by Eqs. (3) and (4) is outside the statically admissible region

Substitution of Eqs. (6) and (7) into (5) gives the following inequality:

$$p - p_0 \left[1 + \left(\frac{r}{a} \right)^2 \sin \varphi \right] \leq 0. \tag{8}$$

The above relation takes the following form at the cavity boundary ($r = a$):

$$p \leq p_0 (1 + \sin \varphi). \tag{9}$$

On the other hand, there should be $p > p_0$ if the process of cavity expansion may take place. Eq. (9) gives a relatively small margin of statically admissible pressure before reaching the Coulomb-Mohr yield condition.

3. Some Heuristic Considerations

Yu (2000) provides an extensive theoreticul discussion of cavity expansion methods. He reviews basic findings and solutions from the world literature, as well as presents his own achievements. However, the question is whether classical models of materials can be directly applied to the problem considered in this paper. For example, the assumption of incompressibility is sometimes adopted, which is physically unrealistic in the case of dynamic nailing. Consider again Fig. 3. During the expansion of the cavity from $r = a$ to $r = b$, the soil mass from region I is displaced to region II. This means that the soil in region II is compacted, so volumetric deformations should be taken into account.

Another problem is that during the dynamic nailing large stresses are applied, which causes partial fracturing of sand grains. It was discovered that a ring, composed of very fine particles, had been formed in front of the cone. This structure collapsed under its own weight during post experimental investigations. Such phenomena are not taken into account by classical models. The grain size distribution in region II (Fig. 3) is probably different from that in region I.

Another question concerns the application of critical state models in the analysis of cavity expansion. Recall that the soil in the critical (or steady) state deforms continuously at constant stresses and volume. This definition of the critical/steady state does not apply to cavity expansion as the constant volume condition is not satisfied, because of the compaction of the soil surrounding the nail. Additionally, it is difficult to imagine a continuous expansion of the cavity under constant pressure, as it is sometimes assumed in purely theoretical considerations. Also note that during the process of nailing, the cavity is expanded by large forces indeed. If their action ceases, the cavity remains as it was before, without any further expansion, and eventually some partial unloading may take place. All these facts severely limit the usefulness of critical/steady state models in the case of cavity expansion in granular media.

A certain shortcoming is that the initial state of the soil is not taken into account in most of theoretical analyses. This initial state may be defined either as contractive or dilative, depending on the position of the point e, p' with respect to the steady-state line (SSL). Here, e = void ratio, p' = mean effective stress. The initial states lying above the steady-state line are considered as contractive, and those below as dilative. In a contractive state, the sand is compacted during shearing, and in a dilative one, it expands while sheared, after a small initial compaction. SSL should be determined experimentally. Interesting possible scenarios are shown in Fig. 5.

Point A corresponds to an initially contractive state of the soil, and point B to an initially dilative one. In both cases, during the cavity expansion, the mean stress increases and the void ratio decreases as a result of compaction. Respective paths can be represented by arrows AB and CD. The steady (or critical) state may occur when points B or D approach SSL, which may never happen. On paths AB and CD shown in Fig. 5 certainly no steady-state conditions are satisfied. The above heuristic discussion suggests that a new and special model of soil should be developed in order to describe realistically the problem considered.

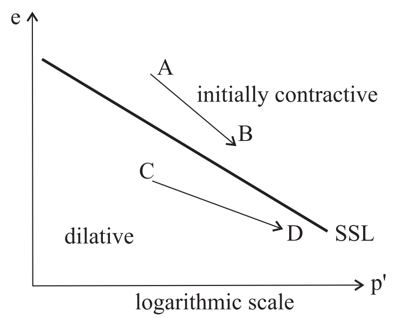

Fig. 5. Possible paths in the e, p' space during cavity expansion

4. Oedometer Analogy

As already mentioned, during cavity expansion in a granular soil, one may expect circumferential stresses to be positive, i.e. compressive, and not negative, as it follows from Eq. (4). An oedometer analogy will be useful to understand the physics of phenomena taking place around the nail.

During cavity expansion, the arc element MN transforms into the arc element M′N′, as shown in Fig. 6. The length of M′N′ is greater than that of MN. In classical mechanics of materials, it is assumed that material particles lying on the arc MN are merely displaced to a new place, defined by the arc M′N′. This assumption may be accepted in the case of an expanding elastic rubber tube, but not in the case of granular matter, as schematically illustrated in Fig. 6. Before incremental deformation, only the particles numbered 1, 2 and 3 occupy the length MN. Particles 4 and 5 lie above the sector MN. After the deformation, these particles are replaced onto the sector M′N′, and additional circumferential stresses are generated to support this new configuration. It bears a certain analogy to partially oedometric conditions, with controlled lateral displacements.

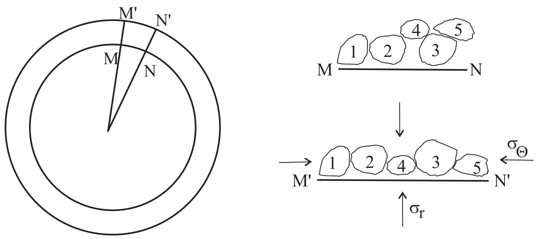

Fig. 6. Re-arrangement of grains during cavity expansion

The above heuristic example shows that some basic principles of continuum mechanics do not apply in the case of granular materials. According to the physical interpretation of a basic assumption known as the strain compatibility, neighbouring points remain neighbours after a deformation. Fig. 6 shows that particles 4 and 5, which had been neighbours before the incremental deformation, were separated by particle 3 after this deformation.

5. Simple Static Solution for Stresses

We are looking for a simple static solution that satisfies the equilibrium equation (2) with respective boundary conditions and takes into account the physical requirement that circumferential stresses should be positive (compressive). Assume that the circumferential stress is proportional to the radial stress:

$$\sigma_\Theta = k\sigma_r, \tag{10}$$

where k is a coefficient of proportionality.

Substitution of Eq. (10) into the equilibrium equation (2) leads to the following differential equation for the radial stress:

$$r\frac{d\sigma_r}{dr} + (1-k)\sigma_r = 0. \tag{11}$$

The solution, with the boundary condition $\sigma_r(r = a) = p$, is the following:

$$\sigma_r = p\left(\frac{a}{r}\right)^{1-k}. \tag{12}$$

Substitution of Eqs. (10) and (12) into the Coulomb-Mohr condition (5) leads to the following inequality, which guarantees that the stress state is statically admissible:

$$k \geq \frac{1-\sin\varphi}{1+\sin\varphi}. \tag{13}$$

In the case when $k = (1-\sin\varphi)/(1+\sin\varphi)$, the stress path coincides with the Coulomb-Mohr line, cf. Fig. 4. Such a value of k is unrealistic as it means that all the soil outside the cavity is in the plastic state (condition (13) is independent of r). It is physically expected that outside the cavity, only a certain ring would remain in the plastic state, but the soil beyond that ring would behave elastically or would remain rigid. Note that when $k = -1$, Eqs. (10) and (12) are the same as (3) and (4). However, $k = -1$ does not satisfy the condition (13), as already mentioned. In the case when $k = 1$, one obtains the hydrostatic stress around the cavity, which is also unrealistic. On the other hand, the latter case corresponds to $\varphi = 0$, which means that the medium is not granular. Therefore, physically sensible values of k are given by the following relation:

$$\frac{1-\sin\varphi}{1+\sin\varphi} < k < 1. \tag{14}$$

This means that only the stress paths similar to those shown in Fig. 4 in a statically admissible region can be realized. Similar stress paths are followed during oedometric experiments, cf. Sawicki and Świdziński (1998). Note that during oedometric tests, the Coulomb-Mohr criterion is not satisfied, but plastic strains develop because of compaction. The static solution, presented in this section allows only for some estimation of stresses generated during the cavity expansion as the value of k is unknown, except for the interval given by relation (14). It should also be noted that Eq. (12) gives a much smaller decrease of radial stress with increasing r than Eq. (6). An analysis of deformations and constitutive relations is necessary in order to get further insight into the problem of cavity expansion in a granular medium.

6. More Advanced Static Solution

The static solutions presented in Sections 2 and 5 will be combined in order to obtain a more realistic stress state around the expanding cavity. Assume that before reaching the Coulomb-Mohr yield condition, stresses are given by Eqs. (6) and (7). This condition is reached when

$$p = p^* = p_0 \left[1 + \left(\frac{r}{a} \right)^2 \sin \varphi \right]. \tag{15}$$

Recall that the loading process starts from the isotropic stress state $p = p_0$, which corresponds to $\sigma_r = \sigma_\Theta = p_0$ (point 1 in Fig. 7). During this stage, the stress path $\sigma_r = -\sigma_0 + 2p_0$ is followed (1–2 in Fig. 7). The Coulomb-Mohr yield condition is attained for the following stresses (point 2 in Fig. 7):

$$\sigma_r^* = \frac{2p_0\Phi}{1+\Phi}, \tag{16}$$

$$\sigma_\Theta^* = \frac{2p_0}{1+\Phi}, \tag{17}$$

where $\Phi = (1 + \sin\varphi)/(1 - \sin\varphi)$, see Fig. 7.

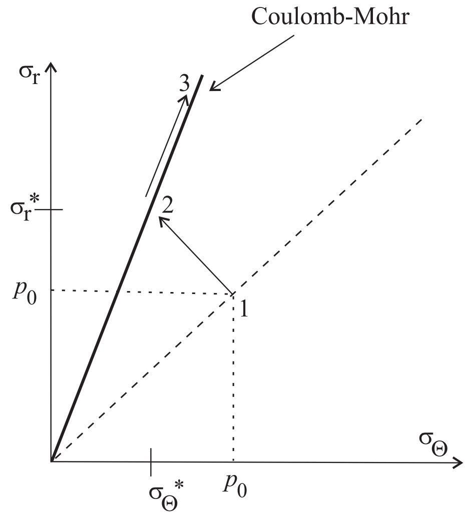

Fig. 7. Stress paths followed during cavity expansion: 1–2 elastic/rigid range; 2–3 plastic behaviour

Further loading is possible only along the Coulomb-Mohr envelope (path 2–3 in Fig. 7). Stress increments along this path should satisfy the following equation:

$$d\sigma_r = \Phi d\sigma_\Theta, \tag{18}$$

as well as the equilibrium equation:

$$\frac{\partial(d\sigma_r)}{\partial r} + \frac{d\sigma_r - d\sigma_\Theta}{r} = 0, \tag{19}$$

where $d()$ denotes an increment of respective quantity.

Integration of Eqs. (19) and (18) with the initial condition at point 2 in Fig. 7 leads to the following stresses:

$$\sigma_r = \sigma_r^* + (p - p^*)\left(\frac{a}{r}\right)^{\beta}, \tag{20}$$

$$\sigma_\Theta = \sigma_\Theta^* + \frac{1}{\Phi}\left[(p - p^*)\left(\frac{a}{r}\right)^{\beta}\right], \tag{21}$$

where $\beta = (\Phi - 1)/\Phi = 2\sin\varphi/(1 + \sin\varphi)$.

7. Kinematics of Cavity Expansion

7.1. Basic Definitions

For small strains, the following classical measures are appropriate:

$$\varepsilon_r = -\frac{\partial u}{\partial r}, \tag{22}$$

$$\varepsilon_\Theta = -\frac{u}{r}, \tag{23}$$

where

- u – radial displacement,
- ε_r – radial strain,
- ε_Θ – circumferential strain.

The minus signs in Eqs. (22) and (23) were introduced according to the soil mechanics convention that compression is positive.

In the case of large strains, various strain measures can be applied. It seems that in the axisymmetrical case considered, logarithmic strain measures are the most appropriate, see Hill (1950), Życzkowski (1973) or Yu (2000). They are defined as follows:

$$\varepsilon_r = -\ln\left(\frac{dr}{dr_0}\right), \tag{24}$$

$$\varepsilon_\Theta = -\ln\left(\frac{r}{r_0}\right), \tag{25}$$

where r_0 denotes the initial position of a chosen point before deformation, r denotes the current position of the same material point after deformation and $d()$ is an increment of respective quantity, see Fig. 8. An advantage of logarithmic strain measures is that they are additive. It follows from Fig. 8 that

$$r = r_0 + u. \tag{26}$$

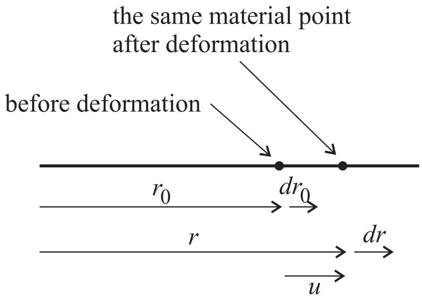

Fig. 8. Kinematics of deformation along radius r

Assume that the character of the radial deformation (u) is known. In such a case, one knows the relation $r = r(r_0)$, from which respective strains can be determined, see Eqs. (24) and (25). A typical continuum mechanics procedure assumes that the system of governing equations, with respective initial and boundary conditions, is known, and the basic problem is to solve these equations in order to determine the strain and stress states. In previous sections, an independent stress analysis was presented, and statically admissible stress fields were determined. In the present section, the kinematics of the deformation is analysed. Subsequently, we shall try to find respective relationships between stresses and strains in order to describe properly the soil behaviour around the nail. In fact, we do not know which constitutive equations are the most appropriate in the case considered, so a typical continuum mechanics procedure cannot be followed.

An important problem is to understand the soil behaviour in the range of large strains and displacements, even for proper interpretation of experimental data. Therefore, some attention will be focused on physical interpretation of large strain measures.

7.2. Interpretation of Large Strains

Assume that the displacement field is known. Usually, this field should be determined from the solution of respective equations with appropriate initial and boundary conditions, but we would like to avoid such an onerous procedure and guess an approximate solution. The following function is a good candidate:

$$u = u_0 \exp(a - r_0) = A_0 \exp(-r_0), \tag{27}$$

where u_0 is the displacement of the boundary of a cylindrical cavity, and a is the initial cavity radius.

Eq. (27) is the simplest function that displays physically expected features of the soil behaviour around an expanding cavity as the radial displacement decreases exponentially with r. Obviously, some modifications of Eq. (27) are possible, but we do not have sufficient experimental data to propose a more realistic relationship. Therefore, let us analyse possible consequences of Eq. (27) and find physical interpretations of large strain measures. Combination of Eqs. (26) and (27) gives the following relation:

$$r = r_0 + A_0 \exp(-r_0). \tag{28}$$

Respective strains are the following:

$$\varepsilon_r = -\ln(1 - A_0 \exp(-r_0)), \tag{29}$$

$$\varepsilon_\Theta = -\ln\left(1 + \frac{A_0}{r_0}\exp(-r_0)\right). \tag{30}$$

In order to show a physical interpretation of the above measures, let us consider a deformation of a cavity defined by the initial radius $r_0 = a = 1$. Assume a large displacement of this cavity defined by $b - a = u_0 = 0.2$, see Fig. 9. Therefore, $A_0 = u_0 \exp(a) = 0.5437$.

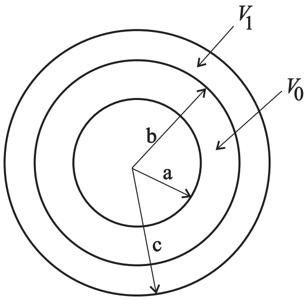

Fig. 9. Large cavity expansion

Note that points lying on the circle $r = a$ were displaced to the new position $r = b$. Respective strains, calculated from Eqs. (29) and (30), are the following: $\varepsilon_r = 0.2232, \varepsilon_\Theta = -0.1823$. The points initially lying on the circle $r_0 = b = 1.2$ were displaced to the position $r = c$. Respective displacement is $u = c - b = 0.5437 \exp(-1.2) = 0.1638$, therefore $c = r = 1.3638$, and the strains are: $\varepsilon_r = -\ln(1 - 0.5437 \exp(-1.2)) = 0.1788, \varepsilon_\Theta = -0.1279$. The average values of these strains are the following: $\varepsilon_r = 0.201, \varepsilon_\Theta = -0.155$. The average volumetric deformation $\varepsilon_v = \varepsilon_r + \varepsilon_\Theta = 0.0459 = 45.9 \times 10^{-3}$.

Consider now a classical definition of volumetric deformation, based on purely geometrical considerations, cf. Fig. 9:

$$\varepsilon_v^{geom} = \frac{V_0 - V_1}{V_0}, \tag{31}$$

where V_0 = area of the ring bounded by $r = a$ and $r = b$, V_1 = respective area bounded by $r = b$ and $r = c$. Elementary calculations lead to the following result: $\varepsilon_v^{geom} =$

45.35×10^{-3}, which is very close to the previous result, namely $\varepsilon_r = 45.9 \times 10^{-3}$. Recall that this latter result was calculated from average values of respective strains.

The radial and circumferential strains defined by Eqs. (22) and (23) lead to the following results for the cavity boundary: $\varepsilon_r = 0.5437 \exp(-1) = 0.2$, versus large strain result of 0.2232; $\varepsilon_\Theta = -0.2/1 = -0.2$ versus -0.1823. For the circle defined by $r_0 = b$, one obtains respectively: $\varepsilon_r = 0.1638$ v. 0.1788 and $\varepsilon_\Theta = -0.1365$ v. -0.1279. Determination of average values of "small strains", as in the case of logarithmic strain measures, and subsequent determination of the average volumetric strain lead to a worse result than in the previous case ($\varepsilon_v = 13 \times 10^{-3}$).

Note that the method applied in this section is a kind of "back analysis", as the displacement field u (Eq. 27) was assumed/guessed, and then the respective strains were calculated. This means that the strain compatibility condition is satisfied automatically. In usual procedures, the strains are determined first, and then respective equations should be integrated in order to determine displacements. In the case of axisymmetrical cavity expansion, a single function u should be determined from two strain functions. That is why the strain compatibility condition should be satisfied.

8. Small Elastic Expansion of Cavity

Consider a small elastic expansion of a cavity corresponding to the stress path 1–2 in Fig. 7. Assume that Hooke's law is valid, i.e.

$$\varepsilon_r = M^* \sigma_r + N^* \sigma_\Theta, \tag{32}$$

$$\varepsilon_\Theta = -N^* \sigma_r + M^* \sigma_\Theta, \tag{33}$$

where $M^* = (1 - \nu^2)/E; N^* = M^* \nu/(1 - \nu)$ and E = Young modulus; ν = Poisson ratio.

The following relation is valid along path 1–2:

$$\sigma_\Theta = -\sigma_r + 2p_0. \tag{34}$$

Substitution of Eqs. (33) and (34) into Eq. (23) leads to the following expression for radial displacement:

$$u = r[(M^* + N^*)\sigma_r - 2M^* p_0]. \tag{35}$$

At the end of stress path 1–2 (point 2 in Fig. 7) and for $r = a$, there is $\sigma_r = \sigma_r^* = p_0(1 + \sin \varphi)$, cf. Eqs. (15) and (16). In this case, the following formula for the cavity displacement is obtained:

$$u_0 = \frac{ap_0(1 + \nu)}{E}[(1 + \sin \varphi) - (1 - 2\nu)]. \tag{36}$$

Assume the following data, which correspond to the average values of parameters characterizing sands: $E = 3 \times 10^8$ N/m^2; $\nu = 0.2; \varphi = 30°$. For $p_0 = 3 \times 10^5$ N/m^2 one obtains the displacement $u_0 = 1.08a \times 10^{-3}$, which is a small value indeed.

An interesting conclusion following from the above simple analysis is that the volumetric strain that develops during the first stage of expansion is equal to zero. There is only an initial uniform volumetric deformation caused by the initial confining stress p_0.

9. Stress – Strain Relations

Up to now, some statically admissible stress fields were determined and an analysis of kinematics around an expanding cavity, including large deformations, was presented. The problem is how to collate these results in order to obtain the relationship between the pressure around the cavity p and its displacement u_0. A simple Coulomb-Mohr condition and classical flow rules are insufficient in this case, as we are not sure whether the soil around the cavity is in the limit state (cf. oedometer analogy discussed in Section 4). No appropriate experimental data have been found in the available literature. It also seems that some of the theoretical models collated by Yu (2000) are not the most appropriate to describe the soil behaviour around the expanding cavity (see some remarks presented in Section 3). All this means that we have to formulate appropriate stress – strain relations for the problem of an expanding cavity.

It is convenient to introduce the following stress and strain measures:

$$p' = \frac{1}{2}(\sigma_r + \sigma_\Theta), \tag{37}$$

$$q = \sigma_r - \sigma_\Theta, \tag{38}$$

$$\varepsilon_v = \varepsilon_r + \varepsilon_\Theta, \tag{39}$$

$$\varepsilon_q = \frac{1}{2}(\varepsilon_r - \varepsilon_\Theta), \tag{40}$$

where p' = mean stress, q = deviatoric stress, ε_v = volumetric strain, ε_q = deviatoric strain. The above quantities satisfy the following relation for the work increment dW:

$$dW = \sigma_r d\varepsilon_r + \sigma_\Theta d\varepsilon_\Theta = p'\varepsilon_v + qd\varepsilon_q. \tag{41}$$

A general form of incremental stress-strain relations for an initially isotropic soil is the following:

$$d\varepsilon_v = Mdp' + Ndq, \tag{42}$$

$$d\varepsilon_q = Qdq, \tag{43}$$

where M, $N$and Q are certain constitutive functions. They may be determined from the assumed flow rule or by other methods. For example, Sawicki and Świdziński (2010a, b) have proposed the following functions on the basis of extensive experimental data obtained from triaxial tests:

$$M = \frac{A_v}{2\sqrt{p'}}, \; N = \frac{4c_1\eta^3}{\sqrt{p'}}, \; Q = \frac{b_1 b_2 \exp(b_2\eta)}{\sqrt{p'}}, \tag{44}$$

where $\eta = q/p'$. Coefficients appearing in Eq. (44) can be found in Sawicki and Świdziński (2010a).

10. Simplified Approach

In the conventional continuum mechanics approach, the full system of governing equations should be solved for given boundary conditions. Because the behaviour of soil is highly non-linear, both physically and geometrically, it is a difficult task that would require a separate paper. On the other hand, it is not clear which model of soil is appropriate in this case, and we do not even know the initial radius of the cavity. Recall that our aim is only to assess radial stresses around the nail. It seems that the cavity expansion method is not a proper approach in this case. Therefore, a simplified, semi-empirical approach is proposed.

This approach is based on the results of experiments described in Sawicki and Kulczykowski (2010). The first set of experiments dealt with pulling nails out, see Fig. 2. Analyses of these experiments have shown that normal stresses around the nail of 16 mm in diameter are of the order of 5 MPa. The second set of experiments were cone penetration tests. Wooden cones were pressed into a sand-filled steel tube, as shown in Fig. 10. At the top of the tube, a steel plate was installed in order to prevent upwards soil deformation. The depth of penetration z and the pressing force P were recorded.

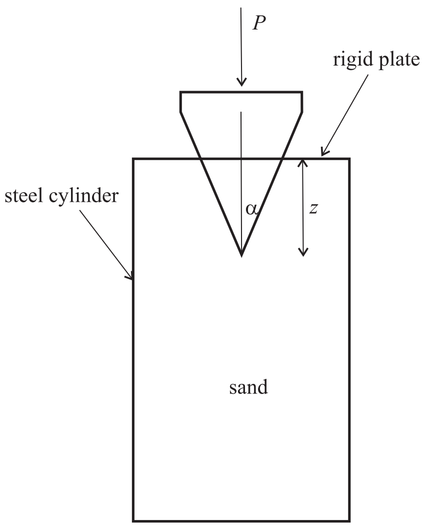

Fig. 10. Cone penetration test – schematic diagram

Fig. 11 shows the relationship between the force P and the depth of penetration z. The following power law approximates experimental results:

$$P = mz^n, \tag{45}$$

where m and n are certain numbers. Fig. 11 corresponds to the experiment in which the cone characterized by the angle $\alpha = 30°$ was used. The maximum diameter of the cone was 50 mm. For these data, there is $m = 3.32 \times 10^{-5}$, $n = 3.42$. Note that P is expressed in newtons (N), and z in mm. Also note that the height of the cone was 43.3 mm, so Fig. 11 covers the whole range of cone penetration, up to the wooden cylinder of 50 mm in diameter. At the beginning of pressing, down to approximately the mid-height of the cone (ca 20 mm), the pressing force is almost negligible, but then increases exponentially. It may be a hint suggesting the possible initial radius of the cavity.

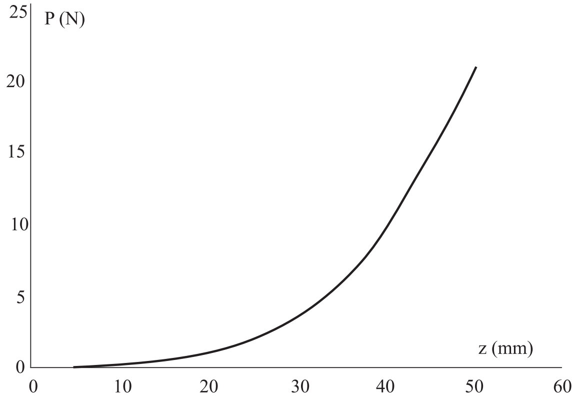

Fig. 11. Relation between the pressing force and the depth of penetration

From the theoretical view point, the cavity expands from the zero initial radius (cone's tip) to its finite size. In such a case, some theoretical solutions admit a constant cavity pressure at which the cavity expands, see Yu (2000), page 125. Such a model can hardly be applied to cavity expansion in granular soils as it is not supported by any experimental observations. Fig. 11 shows that it is increasingly difficult to press the cone into the soil, and no indication exists that there is a limit pressure under which the cavity would expand to infinity.

Eq. (45) suggests that a similar formula can be assumed for the cavity pressure:

$$p = p_0 + A\left(\frac{a}{a_0}\right)^B, \tag{46}$$

where a_0 = initial radius of the cavity, a = final radius of the cavity, A and B are certain coefficients. It is assumed that $B = n = 3.42$, just because of the analogy suggested. It is also assumed that $a_0 = a/2$ because Fig. 11 suggests that the cavity pressure is negligible when the cone penetrates down to the half of its height. These two assumptions, combined with the empirical observations that normal stresses around the nail are of the order of 5 MPa and that the initial confining stress is equal to zero, make it possible to determine A. In this special case, Eq. (46) takes the following particular form:

$$p = 0.467 \times \left(\frac{a}{a_0}\right)^{3.42} \text{(MPa)}. \tag{47}$$

The formulae (46) and (47) are rough approximations of actual normal stresses around the nail, but at the present stage we cannot expect better results. Note that Sikora (2006) offers hardly any hints or solutions as to possible links between cone penetration tests and the cavity expansion method, although he attempts to discuss the main contemporary achievements.

11. Discussion and Conclusions

The aim of this study was to find a method that would make it possible to assess normal stresses around a dynamically driven nail. The cavity expansion method was analyzed as a possible candidate because this approach is often applied in geomechanics in connection with cone penetration tests. The main results can be summarized as follows:

1. Static solutions for cavity expansion were presented. Solutions presented in Section 2 have already been known as almost classical, but solutions presented in Sections 5 and 6 are more advanced and realistic in the case of cavity expansion in granular soils. Statically admissible solutions, i.e. those bounded by the Coulomb-Mohr yield condition, were identified and discussed.
2. Some solutions proposed in literature were discussed. Some of them are based on the critical/steady state models of the soil around the cavity. It seems that the application of such models is vague as during the expansion of the cavity, volumetric strains develop, and the cavity pressure increases. From the definition, during the critical/steady state the soil deforms continuously at a constant volume and constant stresses. This means that there is a contradiction between basic definitions and some analytical approaches. Therefore, the proposed solutions are of little meaning. Another controversial example is the expansion of a cavity from the zero initial radius. In some papers, it was shown that such a cavity expands to infinity at a constant cavity pressure. From the physical point of view, it is difficult to accept such results as the soil surrounding the cavity imposes strong constraints on its expansion.
3. The oedometer analogy presented in Section 4 shows that during the cavity expansion in granular soils one of the basic principles of continuum mechanics, the strain compatibility condition, may be violated., This is obviously no revolutionary discovery, but it may be a hint that this principle should be relaxed in soil mechanics.

4. Another important problem is the kinematics of an expanding cavity. The theory of small strains and displacements is of limited value as these kinematic variables are large during the cavity expansion. Some discussion of this problem is presented in Section 7, where the logarithmic strain measures were introduced.
5. Stress-strain relations are one more important problem. In fact, proper constitutive equations describing the behaviour of the soil around an expanding cavity are not known. As already mentioned, the critical/steady state models are not relevant in this case. General suggestions presented in Section 5 are just a tentative proposal. Their application requires further studies.
6. A simple empirical relation between the normal stress around the nail and the radius of the cavity was proposed. It is the first attempt to find a correlation between the cavity expansion and other factors. The problem is certainly extremely difficult and needs further investigations.

References

Bigoni D., Laudiero F. (1989) The quasi-static finite cavity expansion in a non-standard elasto-plastic medium, *Int. Jnl Mech. Sci.,* **31** (11/12), 825–837.

Carter J. P., Booker J. R., Yeung S. K. (1986) Cavity expansion in cohesive frictional soils, *Geotechnique,* **36** (3), 349–358.

Hill R. (1950) *The Mathematical Theory of Plasticity*, Clarendon Press, Oxford.

Salgado R., Mitchell J. K., Jamiolkowski M. (1997) Cavity expansion and penetration resistance in sand, *Jnl Geotechnical and Geoenvironmental Eng., ASCE*, **123** (4), 344–354.

Sawicki A., Kulczykowski M. (2010) Experimental study on the interaction between a nail and soil, *Czasopismo Techniczne, Środowisko,* **106** (14), 107–120, (in Polish).

Sawicki A., Świdziński W. (1998) Elastic moduli of particulate materials, *Powder Technology*, **96**, 24–32.

Sawicki A., Świdziński W. (2010a) Stress-strain relations for dry and saturated sands, Part I: Incremental model, *Jnl Theoretical and Applied Mechanics*, **48** (2), 309–328.

Sawicki A., Świdziński W. (2010b): Stress-strain relations for dry and saturated sands, Part II: Predictions, *Jnl Theoretical and Applied Mechanics*, **48** (2), 329–373.

Sikora Z. (2006) *Static Cone Penetration, Methods and Applications in Geo-Engineering*, WNT, Warsaw (in Polish).

Su S-H., Liao H-J. (2001) Cavity expansion and cone penetration resistance in anisotropic clay, *Jnl Chinese Institute of Engineers,* **24** (6), 659–671.

Timoshenko S., Goodier J. N. (1951) *Theory of Elasticity*, McGraw-Hill, New York/Toronto/London.

Yu H-S. (2000) *Cavity Expansion Methods in Geomechanics*, Kluwer Academic Publishers, Dordrecht/Boston/London.

Życzkowski M. (1973) *Complex Loads in Plasticity Theory*, PWN, Warsaw (in Polish).